FUSION OF THERMAL INFRARED HYPERSPECTRAL AND VIS RGB DATA USING GUIDED FILTER AND SUPERVISED FUSION GRAPH

Wenzhi Liao[1], *Frieke Van Coillie*[2], *Sidharta Gautama*[1], *Aleksandra Pižurica*[1], *Wilfried Philips*[1]

[1] Ghent University-TELIN-IPI-iMinds, Sint-Pietersnieuwstraat 41, 9000 Ghent, Belgium
Email: {Wliao, Sanja, Sidharta.Gautama, Philips}@telin.ugent.be
[2] FORSIT Research Unit, Ghent University, Coupure Links 653, 9000 Ghent, Belgium
Email: Frieke.Vancoillie@UGent.be

ABSTRACT

Nowadays, advanced technology in remote sensing allows us to get multi-sensor and multi-resolution data from the same region. Fusion of these data sources for classification remains challenging problems. We proposed a novel framework for fusion of low spatial-resolution Thermal Infrared (TI) hyperspectral (HS) and high spatial-resolution RGB data. First, we do super-resolution on TI HS data by using RGB image and guided filter in principal component analysis (PCA) domain. Then, we couple feature extraction and data fusion of spectral features (from TI HS data) and spatial features (morphological features generated on RGB data) through supervised fusion graph. Finally, the fused features are used by SVM classifier to generate the final classification map. Experimental results on the classification of fusing real TI HS and RGB images demonstrate the effectiveness of the proposed method both visually and quantitatively.

***Index Terms*—** Data fusion, multi-resolution, remote sensing, hyperspectral image

1. INTRODUCTION

Recent advances in the sensors technology of remote sensing (RS) have led to an increased availability of acquiring multi-sensor and multi-resolution data from the same area. In particular, hyperspectral (HS) images provide a detailed description of the spectral signatures of ground covers but with low spatial resolution, whereas visual RGB images with high resolution give detailed spatial information the same surveyed area. Many techniques have been developed for fusion of multi-sensor and multi-resolution RS imagery [1–5]. To super-resolve the low spatial resolution HS/multispectral (MS) to the same spatial size of high resolution RGB/panchromatic (PAN) image, some of these approaches employ the so-called component substitution methods [1] or their generalization [2]. Others model PAN image as a linear combination of the ideal MS bands, and restore an ideal high-resolution MS image by utilizing different regularization [3]. Recently, Licciardi et al. [4] combined non-linear PCA (NLPCA) and Indusion to enhance the spatial resolution of the HS image by fusing a PAN image. Their method first applied NLPCA to project the original HS data into a lower space, then enhanced the derived nonlinear PCs by the Indusion process; finally, got the high spatial resolution HS data by inversing NLPCA. However, these approaches either suffer from spectral distortions or from high cost on computational time to estimate a good solution.

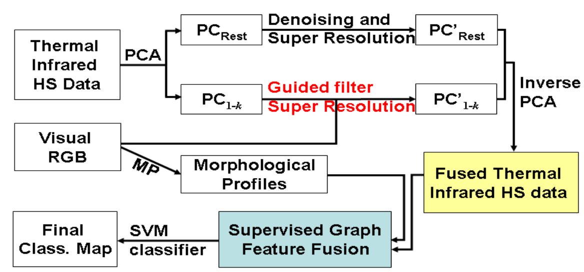

Fig. 1: Proposed framework for super-resolution and data fusion of thermal Infrared hyperspectral and RGB imagery.

For classification tasks, Thoonen et al. [5] proposed composite decision fusion to fuse the classification maps obtained from both a low spatial HS image and a high spatial RGB image using color attribute profiles. However, their method super-resolved HS by just using simply cubic interpolation, which will cause spatial distortions in the classification map. Our graph-based data fusion method won the "Best Paper Challenge" award of 2013 IEEE Data Fusion Contest, but with unsupervised fusion graph [6], which does not take the class discrimination into account.

In this paper, we propose a novel framework for both super-resolution and data fusion of a low spatial resolution Thermal Infrared (TI) HS image and a high spatial RGB image of the same scene. Fig. 1 shows our proposed framework. We first use RGB image and guided filter [7] to do super-resolution of TI HS image in PCA domain, and generate morphological features on original RGB image. Then, we couple dimensionality reduction and data fusion of the spectral information (of super-resolved TI HS image) and the morphological features (computed on RGB image) together with supervised graph-based fusion method. Finally, the fused features are used by SVM classifier to generate the final classification map. Experimental results demonstrate the proposed fusion method can not only preserve the original spectral information and spatial details from RGB image, but also couple dimension reduction and data fusion in a supervised fusion graph for an effective and efficient classification.

2. MORPHOLOGICAL FEATURES OF RGB IMAGE

Morphological features are generated by either applying morphological openings or closings by reconstruction on the image, using a structural element (SE) of predefined size. An opening acts on bright objects compared with their surrounding, while closings act on dark objects. For example, an opening deletes bright objects that are smaller than the SE. By increasing the size of the SE and repeating the previous operation, a complete morphological profile (MP) is built, carrying information about the size and the shape of objects in image.

In our experiments, morphological features are generated by applying morphological openings and closings with partial reconstruction on RGB image. The effect of using morphological features with partial reconstruction for classification of remote sensing data from urban areas has been discussed in our previous work [6, 9]. MPs with 10 openings and closings (ranging from 1 to 10 with step size increment of 1) are computed on RGB image with disk SE.

3. PROPOSED METHOD FOR SUPER-RESOLUTION AND DATA FUSION

3.1. Proposed super-resolution by PCA and guided filter

One of the main challenges of fusion a low spatial HS and a high resolution RGB to get a high spatial resolution HS, is not easy to make a balance on spectral and spatial preservations. Recently, the guided filter [7] has been widely used in many applications (e.g. edge-aware smoothing, detail enhancement and etc.), as its efficient and strong abilities to transfer the structures of the guidance image to the filtering output. Its application to HS data can be found in [8].

In this paper, we propose a novel method to enhance the spatial resolution of TI HS image by using PCA and guided filter. Instead of component substitution which may cause spectral distortions, we use a high resolution RGB image to guided filter the super-resolution of low spatial resolution HS image. By guided filtering the super-resolution process, our method can not only preserve the spectral information from the original HS image, but also transfer the spatial structures of high resolution RGB image to the enhanced HS image. To speed up the processing time, our method first uses PCA to decorrelate the HS images and separate the information content from the noise. The first k PCA channels contain most of

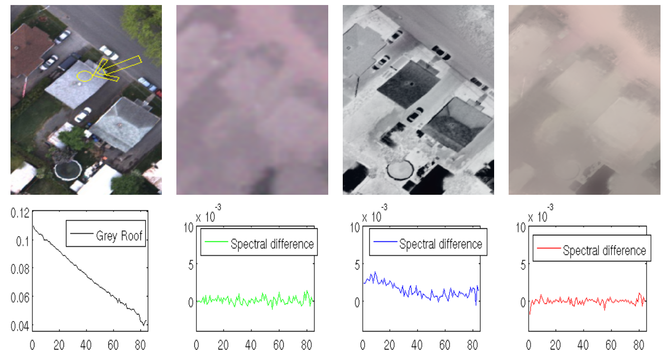

Fig. 2: Part of fused TI HS image. The top row shows RGB image and enhanced images by cubic interpolation, PCA substitution and our proposed method; the second row shows the original spectra from grey roof and its difference with cubic interpolation, PCA substitution and our proposed method.

the total energy of a HS image (i.e. most information of the HS image), and the remaining $B-k$ PCA channels (where B is the number of spectral bands of HSI and $B \gg k$) mainly contain noise. If guided filtering is performed on these noisy and high-dimensional $B-k$ PCs, then it will amplify the noise of the data cube and cause high computational cost in processing the data, which is undesirable. Therefore, we use cubic interpolation and guided filter to only enlarge the first k PCA channels and preserve the structures of RGB image. Let PC_i denote the first i (i) PC after enlarging with cubic interpolation, the filtering output PC_i' can be represented as a linear transform of guided image I_{RGB} in a local window ω of size $(2r+1)\times(2r+1)$ as follows:

$$PC_i' = a_j I_{RGB} + b_j, \forall i \in \omega_j \quad (1)$$

The above model ensures that the output PC_i' has an edge only if the guided image I_{RGB} has an edge, as $\nabla PC' = a\nabla I_{RGB}$. The following cost function was used to find the coefficients a_j and b_j:

$$E(a_j, b_j) = \Sigma_{i\in\omega_j}(a_j I_{RGB} + b_j - PC_i)^2 + \epsilon a_j^2) \quad (2)$$

where ϵ is a regularization parameter determining the degree of the blurring for the guided filter. For more details about guided filter, we refer the readers to [7]. In the cost function, the $PC_i' = a_j I_{RGB} + b_j$ should be as close as much to the PC_i, which can make sure the preservation of the original spectral information. We remove the noise in the remaining PCA channels using a soft-thresholding scheme and enlarge their spatial sizes to the same as the RGB image only using cubic interpolation (and without guided filter). Fig. 2 shows the effectiveness of our proposed image fusion method in spectral and spatial preservations.

3.2. Proposed Graph Embedding Fusion Method

Using single data source may not be sufficient for a reliable classification, but combining many of them can lead to problems like the curse of dimensionality, excessive computation time and so on. We proposed a graph-based data fusion method [6] to fuse hyperspectral and LiDAR data for classification, but with unsupervised fusion graph. In this paper, we extend it to supervised version, which take into account class discrimination. Let $\mathbf{X}^{HS} = \{\mathbf{x}_i^{HS}\}_{i=1}^n$, $\mathbf{X}^{MPs} = \{\mathbf{x}_i^{MPs}\}_{i=1}^n$ and $\mathbf{Y} = \{y_i\}_{i=1}^n$ denote the spectral features after our proposed super-resolution, MPs computed on original RGB image, and the class labels (where $y_i \in \{1, \cdots, C\}$, C is the number of classes), respectively. $\mathbf{X}^{Sta} = \{\mathbf{x}_i^{Sta}\}_{i=1}^n = [\mathbf{X}^{HS}; \mathbf{X}^{Mps}]$ denotes the vector stacked by the spectral and spatial features.

We assume all data sources are scaled to the same ranges before fusion. We first build a graph for each data source, for example, the graph constructed by our super-resolved HS (i.e., $\mathbf{G}^{HS} = (\mathbf{X}^{HS}, \mathbf{A}^{HS})$), where $\mathbf{A}^{HS}$ represents the edges of the graph. The edge between data point $\mathbf{x}_i^{HS}$ and $\mathbf{x}_j^{HS}$ is here denoted as $A_{ij}^{HS} \in \{0, 1\}$; $A_{ij}^{HS} = 1$ if $\mathbf{x}_i^{HS}$ and $\mathbf{x}_j^{HS}$ are "close" and $y_i = y_j$, whereas $A_{ij}^{HS} = 0$ if $\mathbf{x}_i^{HS}$ and $\mathbf{x}_j^{HS}$ are "far apart" or $y_i \neq y_j$. The "close" is defined as belonging to K nearest neighbors (KNN) of the other data points. The KNNs of the data point $\mathbf{x}_i^{HS}$ are its K nearest neighbors in terms of spectral signatures. On the other hand, when the graph is constructed by MPs, the KNNs of the data point $\mathbf{x}_i^{MPs}$ are its K nearest neighbors in terms of spatial characteristics. We define a fusion graph $\mathbf{G}^{Fus} = (\mathbf{X}^{Sta}, \mathbf{A}^{Fus})$, where $\mathbf{A}^{Fus} = \mathbf{A}^{HS} \bigodot \mathbf{A}^{MPs}$. The operator '$\bigodot$' denotes element-wise multiplication, i.e. $A_{ij}^{Fus} = A_{ij}^{HS} A_{ij}^{MPs}$.

$$A_{ij}^{Fus} = \begin{cases} 1 & \text{if } A_{ij}^{HS} \bigwedge A_{ij}^{MPs} = 1 \text{ and } y_i = y_j \\ 0 & \text{if } A_{ij}^{HS} \bigvee A_{ij}^{MPs} = 0 \text{ or } y_i \neq y_j \end{cases}$$

This means that the stacked data point $\mathbf{x}_i^{Sta}$ and $\mathbf{x}_j^{Sta}$ are connected only if they have similar both spectral and spatial characteristics and they are from the same class. For more details to obtain the fused features, we refer the readers to our recent work reported in [6].

4. EXPERIMENTAL RESULTS

Experiments are done on a thermal infrared hyperspectral data and a visual RGB image which were acquired by Telops Inc. on May 2013 over an urban area near Thetford Mines in Québec, Canada. The TI HS image has 84 spectral bands that covers the wavelengths between 7.8 to 11.5 μm with approximately 1-m spatial resolution. The visible RGB image is a series of color images acquired during separate flight-lines with approximately 20-cm spatial resolution. The whole scene of both data contains 7 classes, but with different spatial size of which the TI HS consists of 874×751 pixels while RGB of 4386×3769. Fig. 3 shows an RGB composition with the labeled classes highlighted, for details, see [10].

The SVM classifier with radial basis function (RBF) kernels is applied in our experiments. We apply a grid-search on the two parameters C and γ of SVM using 5-fold cross-validation to find the best C within the given set $\{10^{-1}, 10^0, 10^1, 10^2, 10^3\}$ and the best γ within the given set $\{10^{-3}, 10^{-2}, 10^{-1}, 10^0, 10^1\}$. We compare our proposed fusion method (SGF) with the schemes of (1) Simply enlarging the original HS image by cubic interpolation (Cub); (2) PCA component substitution method (PCA), similar as [1]; (3) Our proposed image fusion using guided filter in PCA domain (GFP); (4) Using MPs computed on original RGB image (MPs); (5) Stacking our enhanced HS image and MPs (Sta); (6) Unsupervised graph-based fusion method (UGF) [6] to fuse our enhanced HS image and MPs. For quantitative comparisons, we divide all labeled samples spatially isolated into two equal groups, one group for training set, the other for test. Within the training set, we randomly select 1000 samples per class for training, the results are averaged over five runs. The classification results are quantitatively evaluated by measuring the Overall Accuracy (OA), the Average Accuracy (AA) and the Kappa coefficient (κ) on the test data. The experiments were carried out on 64-b, 3.40 GHz Intel i7-4930K (1 core) CPU computer with 64 GB memory, the consumed time includes image fusion, feature fusion and classification. Table 1 shows the accuracies and consumed time (hours) obtained from the experiments, Fig. 3 shows the best result of each method.

Table 1: Average classification accuracies and consumed time (hour) obtained according to the described scheme.

	Cub	PCA	GFP	MPs	Sta	UGF	SGF
Feat.	84	84	84	60	144	23	18
OA (%)	78.1	78.8	91.6	88.7	90.6	93.2	**96.7**
AA (%)	72.4	73.9	84.7	86.4	87.3	90.7	**96.6**
κ (%)	72.8	73.8	89.5	87.8	88.9	91.5	**95.9**
Time (h)	3.81	2.82	1.17	0.67	6.86	0.61	**0.53**

It can be found that our proposed feature fusion method perform better than the others fusion schemes, with more than 3% improvements in accuracies and less consumed time. It is obvious that using single data source is not enough for reliable classification. For example, the spatial information of classes 'Red roof' and 'Grey roof' or 'Bare soil' is similar, objects from 'Red roof' are misclassified as soil by only using MPs. While spectral information from image fusion by the schemes (1) and (2) suffered either spectral distortions or spatial distortions. By using guided filter, the proposed SGF image fusion method performs better on both spectral and spatial preservations, and benefits its classification accuracies with 12.5%-3% improvements than the schemes (1), (2) and (4).

Data fusion by simply stacking different data sources performs even worse than using single data source, but cost more computational time on classification due to the high dimension of stacking features. By taking the class discrimination into account, the proposed supervised graph fusion method performs better than the others, with more than 4% κ improvements over unsupervised graph-based fusion. Moreover, the number of extracted fused features are less than the others, which benefits less consumed time in the process of

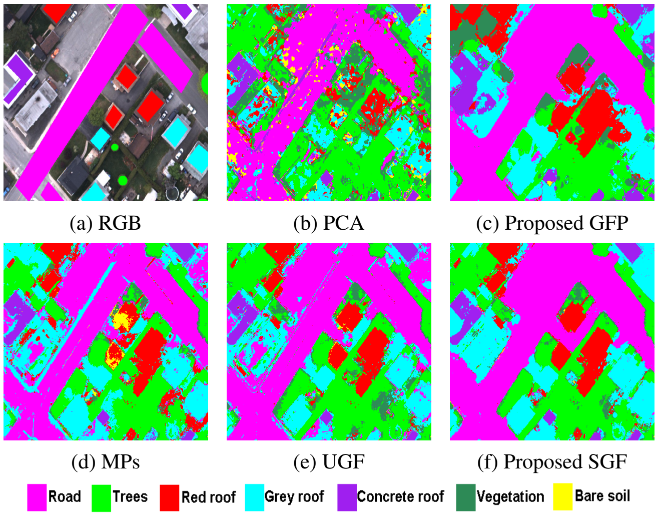

Fig. 3: Part of classification maps obtained by each method.

classification.

5. CONCLUSION

The contribution of this paper is a methodology to fuse a low spatial resolution HS image and a high resolution RGB image in the classification task. Some existing image fusion methods suffer either spectral distortions or spatial distortions. Our proposed image fusion method can preserve both spectral and spatial information by using RGB image and guided filter in PCA domain. Our supervised graph-based fusion considers the class discrimination to couple dimension reduction and data fusion, it can make full advantage of each data sources and reduce the computational cost for classification. Experimental results on the classification of the real TI HS and RGB images show the efficiency of the proposed method.

Acknowledgment

This work was financially supported by the SBO-IWT project Chameleon: Domain-specific Hyperspectral Imaging Systems for Relevant Industrial Applications. The authors would like to thank Telops Inc. (Québec, Canada) for acquiring and providing the data used in this study, the IEEE GRSS Image Analysis and Data Fusion Technical Committee and Dr. Michal Shimoni (Signal and Image Centre, Royal Military Academy, Belgium) for organizing the 2014 Data Fusion Contest, the Centre de Recherche Public Gabriel Lippmann (CRPGL, Luxembourg) and Dr. Martin Schlerf (CRPGL) for their contribution of the Hyper-Cam LWIR sensor, and Dr. Michaela De Martino (University of Genoa, Italy) for her contribution to data preparation.

6. REFERENCES

[1] V. Shah, N. Younan, and R. King, “An efficient pansharpening method via a combined adaptive PCA approach and contourlets,” IEEE Trans. Geosci. Remote Sens., vol. 46, no. 5, pp. 1323–1335, May 2008.

[2] B. Aiazzi, S. Baronti, and M. Selva, “Improving component substitution pansharpening through multivariate regression of MS + Pan data,” IEEE Trans. Geosci. Remote Sens., vol. 45, no. 10, pp. 3230–3239, Oct. 2007.

[3] S. Li, H. Yin, and L. Fang, “Remote sensing image fusion via sparse representations over learned dictionaries,” IEEE Trans. Geosci. Remote Sens., vol. 51, no. 9, pp. 4779–4789, Sep. 2013.

[4] G. Licciardi, M. M. Khan, J. Chanussot, A. Montanvert, L. Condat and C. Jutten: “Fusion of hyperspectral and panchromatic images using multiresolution analysis and nonlinear PCA band reduction,” EURASIP J. Adv. Sig. Proc., vol. 2012 no. 207, pp. 1–17, 2012.

[5] G. Thoonen, Z. Mahmood, S. Peeters, P. Scheunders, “Multisource classification of color and hyperspectral images using color attribute profiles and composite decision fusion,” IEEE journal of selected topics in applied earth observation and remote sensing, vol. 5, no. 2, pp. 510-521, April 2012.

[6] C. Debes, A. Merentitis, R. Heremans, J. Hahn, N. Frangiadakis, T. Kasteren, W. Liao, R. Bellens, A. Pizurica, S. Gautama, W. Philips, S. Prasad, Q. Du, F. Pacifici, “Hyperspectral and LiDAR Data Fusion: Outcome of the 2013 GRSS Data Fusion Contest,” IEEE Journal of Selected Topics in Applied Earth Observations and Remote Sensing, 2014. (In Press).

[7] K. He, J., and X. Tang, “Guided Image Filtering,” IEEE Transactions on Pattern Analysis and Machine Intelligence, vol. 35, no. 6, pp. 1397–1409, 2013

[8] X. Kang, S. Li, J. A. Benediktsson, “Spectral-spatial hyperspectral image classification with edge-preserving filtering,” IEEE Transactions on Geoscience and Remote Sensing. vol. 52, no. 5, pp. 2666-2677, May, 2014.

[9] W. Liao, R. Bellens, A. Pižurica, W. Philips and Y. Pi, “Classification of Hyperspectral Data Over Urban Areas Using Directional Morphological Profiles and Semi-Supervised Feature Extraction,” IEEE Journal of Selected Topics in Applied Earth Observations and Remote Sensing, vol. 5, no. 4, pp. 1177–1190, Aug. 2012.

[10] 2014 IEEE GRSS Data Fusion Contest, Online: *http://www.grss-ieee.org/community/technical-committees/data-fusion-contest/*.